



## Effects of deposition parameters on HFCVD diamond films growth on inner hole surfaces of WC–Co substrates

Xin-chang WANG, Zi-chao LIN, Bin SHEN, Fang-hong SUN

School of Mechanical Engineering, Shanghai Jiao Tong University, Shanghai 200240, China

Received 8 April 2014; accepted 29 July 2014

**Abstract:** Deposition parameters that have great influences on hot filament chemical vapor deposition (HFCVD) diamond films growth on inner hole surfaces of WC–Co substrates mainly include the substrate temperature ( $t$ ), carbon content ( $\varphi$ ), total pressure ( $p$ ) and total mass flow ( $F$ ). Taguchi method was used for the experimental design in order to study the combined effects of the four parameters on the properties of as-deposited diamond films. A new figure-of-merit (FOM) was defined to assess their comprehensive performance. It is clarified that  $t$ ,  $\varphi$  and  $p$  all have significant and complicated effects on the performance of the diamond film and the FOM, which also present some differences as compared with the previous studies on CVD diamond films growth on plane or external surfaces. Aiming to deposit HFCVD diamond films with the best comprehensive performance, the key deposition parameters were finally optimized as:  $t=830$  °C,  $\varphi=4.5\%$ ,  $p=4000$  Pa,  $F=800$  mL/min.

**Key words:** hot filament chemical vapor deposition diamond film; inner hole surface; Taguchi method; deposition parameter; optimization

### 1 Introduction

CVD diamond films have outstanding properties, most notably high hardness, high wear resistance and low friction coefficient that approach single crystal natural diamonds, which make them good candidate protective coatings on working surfaces of wear resistant components. In many cases, such working surfaces are inner hole surfaces (e.g., drawing dies, valves and nozzles [1–3]). The diamond film growth on the inner hole surface puts forward higher requirements for the deposition technology and parameters. Among different types of CVD technologies, the HFCVD method has attracted the most interests because of its advantages like the geometric simplification, low cost and operational convenience, especially the practicality on complicated, large-area and inner hole surfaces [4,5].

Since the successful heteroepitaxy growth of CVD diamond films, the effects of the deposition parameters have drawn the attention of many researchers, serving as the core technology in diamond films growth on different substrates. GUO and CHEN [6] have studied the effects of the gas composition, substrate temperature, gas flow

rate and reactor pressure on HFCVD diamond films growth on Ti substrates and determined the optimal condition so as to obtain high-quality films. RATS et al [7] have evaluated the temperature dependence of the total residual stress of MPCVD diamond films deposited respectively on Ti and Ti–6Al–4V substrates. Similar researches have also been conducted by MAY et al [8], AMARAL et al [9,10] and LI et al [11].

With the development of pretreatment methods, tungsten carbide materials have received more and more attention as substrates to deposit diamond films due to their widespread applications in mechanical, petrochemical and some other fields. The key deposition parameters, such as the filament-substrate separation [12], the temperature [13] and the total pressure [14], play determinate roles in the growth and properties of WC-based diamond films. Nevertheless, related studies on different substrates are mainly focused on diamond films growth on plane or external surfaces [15–18]. During the deposition processes of HFCVD diamond films on inner hole surfaces of WC–Co substrates, similar deposition parameters may have different effects, as a result of the limitation of reaction zone (inner holes), which require further and systematical studies. Besides,

it is also imperative to study the influences of the main deposition parameters on not only the growth and fundamental properties of as-deposited diamond films but also additional properties related to the applications, for instance, the adhesion and wear behavior.

In the present work, Taguchi method was adopted for the experimental design to study the combined effects of the substrate temperature ( $t$ ), carbon content ( $\varphi$ ), total pressure ( $p$ ) and total mass flow ( $F$ ) on the properties of as-deposited HFCVD diamond films on commonly used WC–6%Co (mass fraction) substrates, including the growth rate ( $R$ ), grain size ( $G$ ), total residual stress ( $\sigma$ ), structural quality ( $Q$ ), adhesion ( $\delta$ ) and steady-state wear rate in the wear test ( $I_{da}$ ). Furthermore, a figure-of-merit (FOM) was proposed to assess the comprehensive performance of as-deposited diamond films and the deposition parameters are accordingly optimized.

## 2 Experimental

### 2.1 Deposition and characterization

WC–6% Co hollow cylinder samples ( $d22 \text{ mm} \times 18 \text{ mm}$ ) with an aperture of  $d4.0 \text{ mm}$  were adopted as substrates. Prior to the deposition, all of the substrates were submitted to a two-step alkali-acid pretreatment process in order to remove the binder phase (Co) from the surfaces [19]. Deposition processes were carried out in a vacuum reactor with the mixture of methane and excessive hydrogen as the reactant gas. A  $d0.5 \text{ mm} \times 70 \text{ mm}$  tantalum wire was adopted as the hot filament, being dragged through the inner hole by high temperature springs and located in the center.

Taguchi method was adopted for the experimental design with several significant factors that affect the properties of HFCVD diamond films so that as much useful information as possible can be extracted from a predetermined and limited number of experiments. Four deposition parameters were chosen as factors, including the substrate temperature ( $t$ ), carbon content ( $\varphi$ ), total pressure ( $p$ ) and total mass flow ( $F$ ). Three levels were

chosen for each factor, as shown in Table 1. An L9 ( $3^4$ ) Taguchi array was applied to designing nine deposition conditions, as listed in Table 2. In our previous studies [20,21], the influences of deposition parameters, filament arrangements and heat transfer conditions on substrate temperature values and distributions have been discussed. At present, the substrate temperature was indirectly real-time measured by a high-precision thermocouple placed contacting to the external surface of the substrate. By adopting the simulation method [20], correspondences between  $t$  and measured values were obtained as: 830–760 °C; 750–700 °C; 910–830 °C. The substrate temperature in this work was determined by the filament power so that  $t$  actually means a filament-and-substrate temperatures system. The methane and hydrogen were respectively introduced into the reactor, the mass flow of which was controlled by two mass flowmeters so that parameters  $\varphi$  and  $F$  can be accurately fixed. Moreover,  $p$  is dependent on the total mass flow and the pumping rate provided by the vacuum pump.

**Table 1** Chosen HFCVD parameters and corresponding levels

Parameter	Level 1	Level 2	Level 3
Substrate temperature, $t / ^\circ\text{C}$	830±10	750±10	910±10
Carbon content, $\varphi / \%$	3	1.5	4.5
Total pressure, $p / \text{Pa}$	4000	1600	6000
Total mass flow, $F / (\text{mL} \cdot \text{min}^{-1})$	800	600	1000

Adopting the deposition parameters listed in Table 2, diamond coated samples were firstly fabricated in a constant duration of 5 h. Furthermore, due to the fact that the film thickness plays an important role in the grain size, residual stress and adhesion, diamond coated samples with the same film thickness ( $\sim 20 \mu\text{m}$ ) were also obtained by controlling the deposition duration in order to conduct the performance comparisons at the same level. The field emission scanning electron microscope

**Table 2** L9 ( $3^4$ ) Taguchi array of deposition conditions and analysis results

No.	$t / ^\circ\text{C}$	$\varphi / \%$	$p / \text{Pa}$	$F / (\text{mL} \cdot \text{min}^{-1})$	$R / (\mu\text{m} \cdot \text{h}^{-1})$	$G / \mu\text{m}$	$\sigma / \text{MPa}$	$Q / \%$	$\delta / \text{min}$	$I_{da} / (10^{-6} \text{mg} \cdot \text{N}^{-1} \cdot \text{m}^{-1})$
1	830±10	3	4000	800	4.201	7.076	−1.327	44.17	20	2.72
2	830±10	1.5	1600	600	2.026	2.887	−2.954	19.45	12	8.74
3	830±10	4.5	6000	1000	5.118	7.019	−2.411	47.25	18	2.54
4	750±10	3	1600	1000	4.628	8.148	−2.145	8.38	16	6.18
5	750±10	1.5	6000	800	2.051	10.25	−0.533	7.11	30	6.86
6	750±10	4.5	4000	600	4.353	3.975	−1.149	23.94	20	4.14
7	910±10	3	6000	600	4.219	3.616	−2.012	16.57	18	4.92
8	910±10	1.5	4000	1000	2.324	6.342	−1.522	4.29	16	7.88
9	910±10	4.5	1600	800	5.317	1.917	−4.315	9.61	2	10

(FESEM, Zeiss ULTRA55) was used to observe the cross-sectional morphologies of the films fabricated with the same duration, as well as surface morphologies of the films with the same thickness. The latter ones were also characterized by the Raman spectroscopy using a He–Ne laser with an excitation wavelength of 632.8 nm.

## 2.2 Wear test

An inner hole polishing apparatus was employed to study adhesions and wear rates of as-fabricated diamond coated samples with the same film thickness, by means of a wear test that simulates the application condition of the drawing die. A low-carbon steel wire with a diameter of  $d4.3$  mm was plugged into the inner hole ( $d4.0$  mm) of the diamond coated sample with an interference fit. In the wear test, the wire slid along the axial direction at a linear velocity  $v$  of 0.3 m/s, meanwhile, the coated sample rotated at a constant rotational velocity  $\omega$  of 300 r/min. It was assumed that wears of the wires when sliding against the different samples are the same and have no effects on the loading conditions between the wires and diamond films. Based on the elastic-plastic mechanics, the initial radial load between the wire and the film with an interference fit of 0.3 mm was approximately simulated and defined as 3400 N, which was recognized as a constant in the whole test and adopted to calculate the steady-state wear rate  $I_{da}$  ( $10^{-6}\text{mg}/(\text{N}\cdot\text{m}^{-1})$ ). Mass losses

of the coated samples were measured by a precision balance with  $\pm 0.01$  mg accuracy every 2 min. Before each the measurement, ultrasonic was used to clean up the wear debris on the inner hole surfaces.

## 3 Results and discussion

### 3.1 Growth rate and grain size

Cross-sectional morphologies of the diamond coated samples fabricated with the same duration (5 h) are all presented in Fig. 1, which were obtained by quartering the samples with the low speed wire cutting. The growth rate ( $R$ ) of the film equals the average film thickness over the deposition duration. The average film thickness was obtained by averaging the film thicknesses at four different points. The grain size ( $G$ ) of the diamond crystals is calculated by statistically analyzing surface morphologies of the diamond films with the same thickness ( $\sim 20$   $\mu\text{m}$ ) also at four different points. Figure 2 shows the typical surface morphologies for each diamond film at one of the four points. Under all the conditions, continuous microcrystalline diamond films are fabricated. The calculated values are all listed in Table 2 and the influences of the four controllable factors and corresponding ranges are illustrated in Fig. 3.

The discussion related to  $G$  can refer to an equation as stated below:

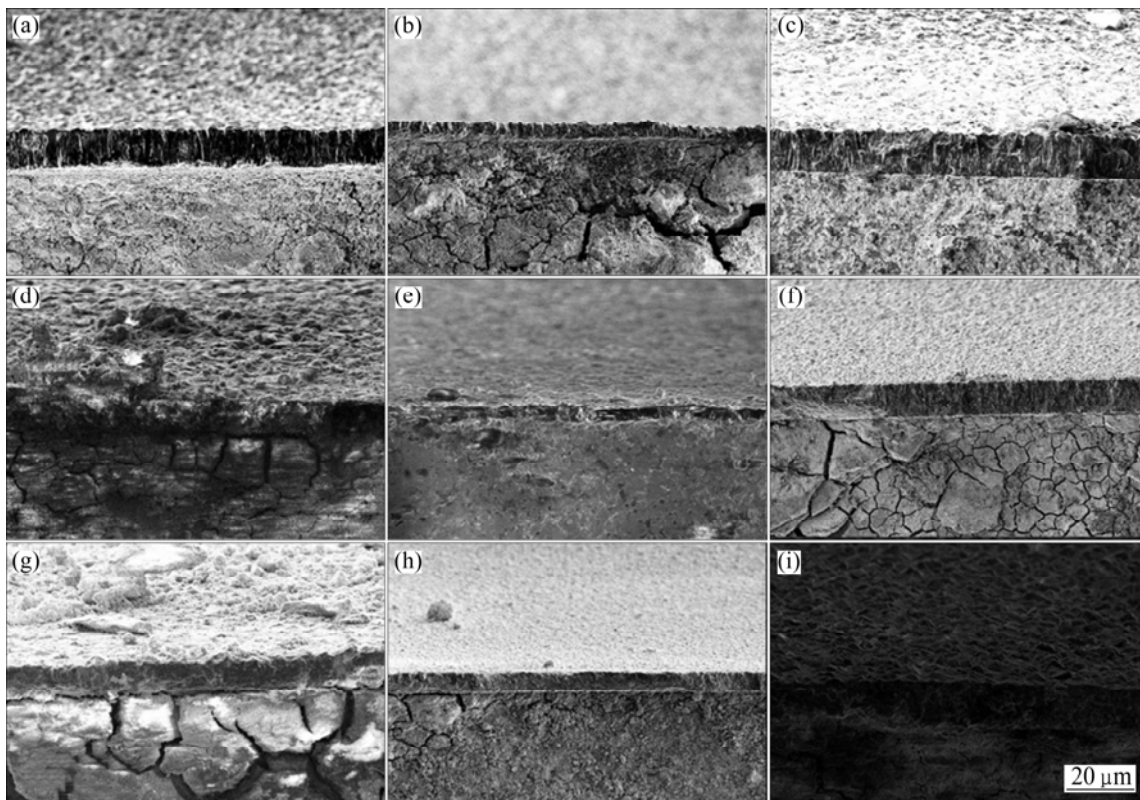


**Fig. 1** Cross-sectional morphologies of diamond coated samples fabricated with same duration of 5 h: (a) No. 1; (b) No. 2; (c) No. 3; (d) No. 4; (e) No. 5; (f) No. 6; (g) No. 7; (h) No. 8; (i) No. 9

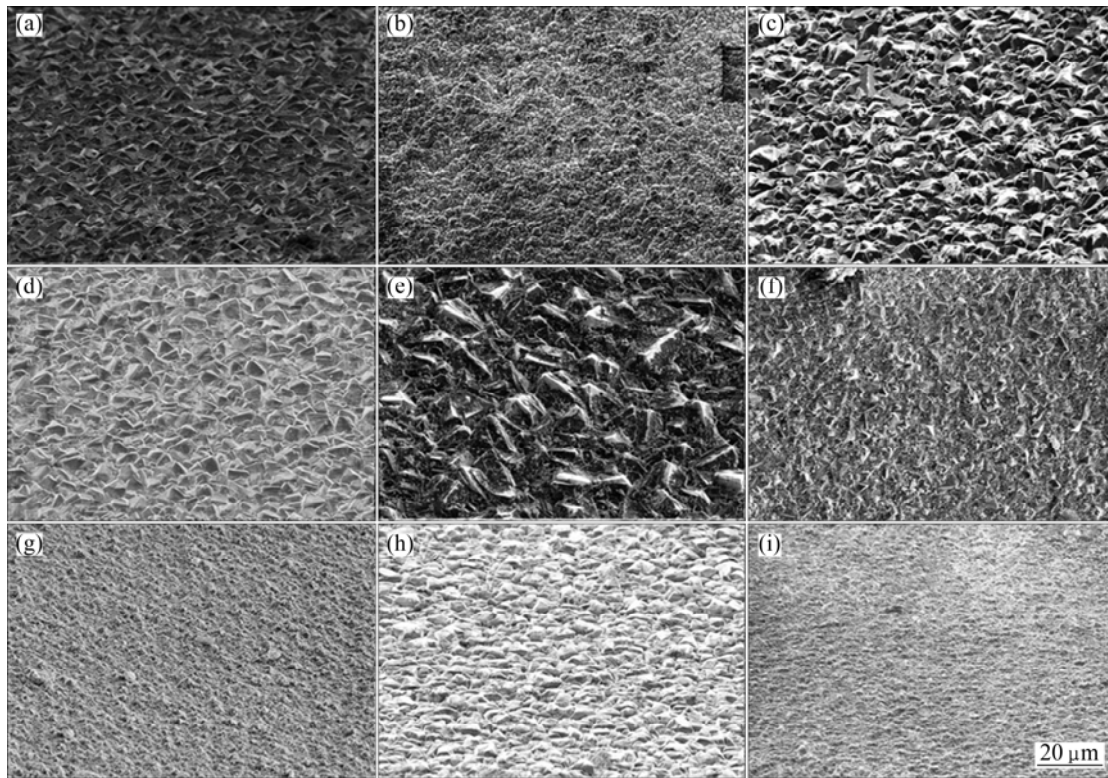


**Fig. 2** Surface morphologies of diamond coated samples with same thickness: (a) No. 1; (b) No. 2; (c) No. 3; (d) No. 4; (e) No. 5; (f) No. 6; (g) No. 7; (h) No. 8; (i) No. 9

$$G = \frac{0.285 \times 3.8 \times 10^{-14} t^{0.5} x(\text{CH}_x)}{1 + 0.3e^{3430/t} + 0.1e^{(-4420/t)} \frac{x(\text{H}_2)}{x(\text{H})}} \quad (1)$$

where  $x(\text{CH}_x)$ ,  $x(\text{H}_2)$  and  $x(\text{H})$  are the concentrations of  $[\text{CH}_x]$ ,  $[\text{H}_2]$  and  $[\text{H}]$ , respectively.

This equation presents kinetic Monte Carlo studies of CVD diamond growth [12,22,23] and approximate qualitative relationships between  $G$  and the mentioned factors are illustrated in Fig. 4, in the estimated ranges of three key factors in the present work.

Firstly, it can be observed from Fig. 3(e<sub>2</sub>) that the dependence of the growth rate ( $R$ ) on the carbon content ( $\varphi$ ) is significant, with a range as high as 2.795. Similar conclusions can also be directly obtained from Table 2 and Fig. 1, showing that under the highest  $\varphi$  (4.5% for experimental Nos. 3, 6 and 9), much thicker diamond films are fabricated in the same duration, indicating higher  $R$ , and exactly the opposite is obtained under the lowest  $\varphi$  (1.5% for experimental No. 2, No. 5, No. 8). It has been discussed by WEI et al [12] that  $G$  scales roughly linearly with  $\varphi$  at small filament–substrate distance but is rather insensitive to  $\varphi$  at large filament–substrate distance [12]. In the present work, the filament–substrate distance is as small as 1.75 mm, so it is supposed that the rise in  $\varphi$  can provide much more sufficient carbonaceous organic material close to the hot

filament and the substrate surface, inducing an obvious increase in the content of methyl radicals ( $[\text{CH}_3]$ ), which is considered the main source for diamond films growth [24,25]. As long as the  $x(\text{H})/x(\text{CH}_3)$  ratio remains relatively high with  $\varphi$  in a reasonable range (e.g., 1.5%–4.5%),  $[\text{CH}_3]$  is a key growth radical in the  $\text{CH}_4\text{--H}_2$  hot-filament system (as demonstrated in Fig. 4), so that the rise of  $\varphi$  can result in a significant increase in  $R$  [26,27]. On the contrary, the increase in  $[\text{CH}_3]$  close to the substrate surface can also promote the nucleation of diamond crystals, for which a great number of small diamond crystals exist in the diamond film and thus for the diamond films with the same thickness, the grain size ( $G$ ) can be reduced with increasing  $\varphi$ , as shown in Fig. 3(e<sub>2</sub>).

Figure 3 also highlights the certain influences of the substrate temperature ( $t$ ) on  $R$  and  $G$ , as illustrated in Fig. 3(e<sub>1</sub>) and (f<sub>1</sub>). It is obvious that  $t$  presents influences on  $R$  and  $G$  similar to  $\varphi$ , which should be attributed to its positive role in promoting the reaction rate of the gas. It has been mentioned above that in this work,  $t$  means a filament-and-substrate temperature system, so the increase in  $t$  is dependent on the enhancement of the electrical power of the hot filament and meanwhile the filament temperature also significantly rises.  $R$  is mainly determined by two reaction processes on the substrate surface: the deposition of carbon radicals and the etching

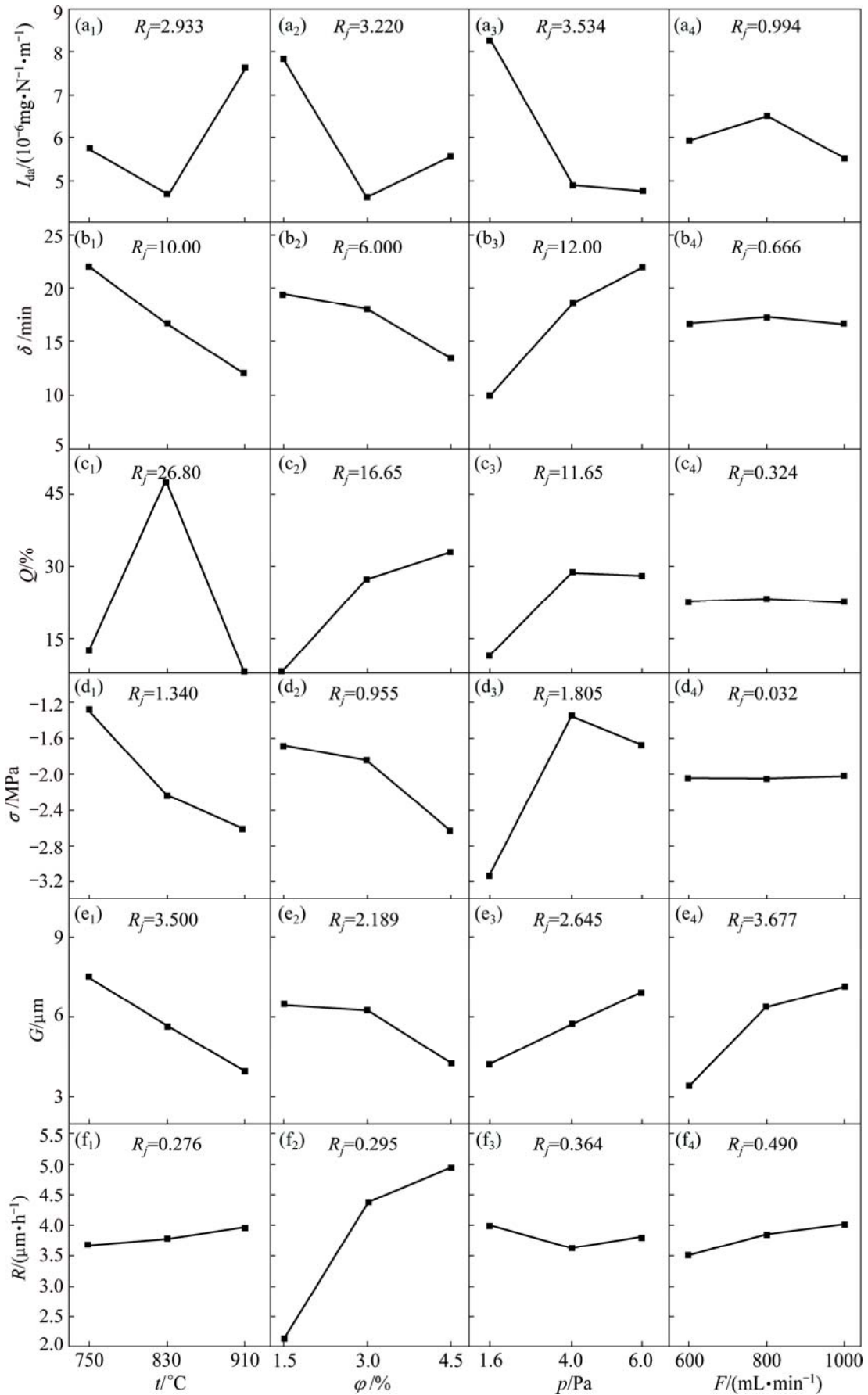
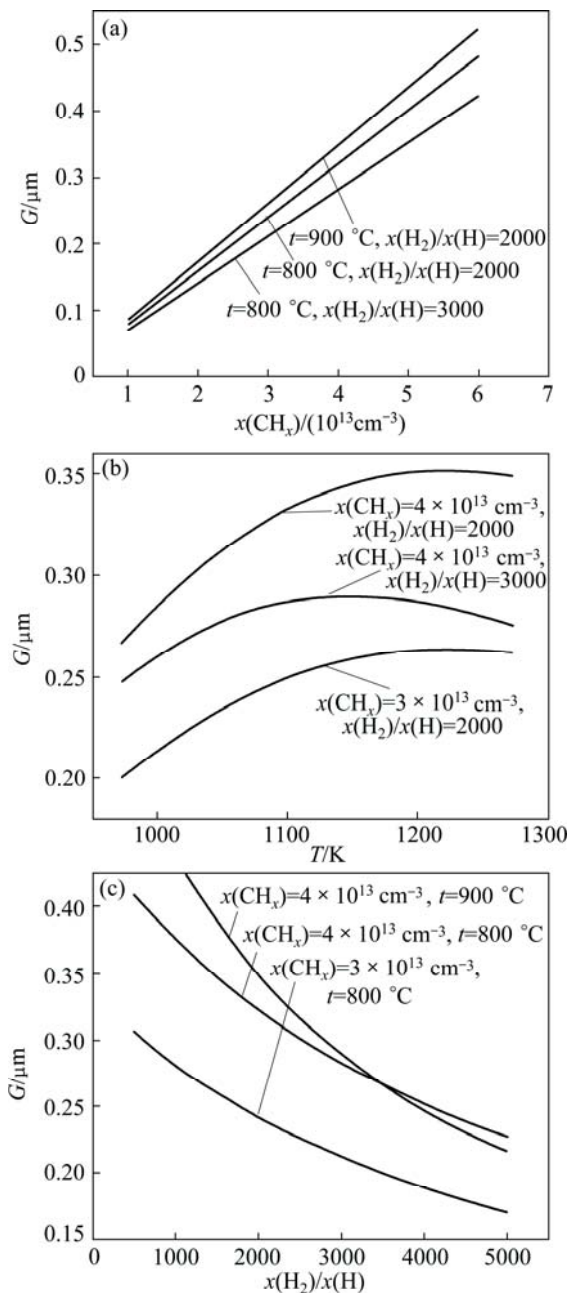


Fig. 3 Influences of controllable factors on indexes and corresponding ranges



**Fig. 4** Approximate qualitative relationships between  $G$  and mentioned three key factors calculated with theoretical equation

effect of [H] atoms on the graphitic phase. In the diamond film growth on the inner hole surface, the filament–substrate distance is 1.75 mm, so under the higher  $t$  condition, more [H] and  $[\text{CH}_3]$  radicals produced by the activation of the filament with higher temperature [10,25] can quickly move to the substrate surface almost without hindrance, leading to an improvement for both the reaction processes. As a result, the increase in  $t$  also induces a slight increase in  $R$  [10], being well consistent with Fig. 4. Moreover, it has been proved that the nucleation densities of the diamond will increase with

the substrate temperature in an appropriate range and reach the maximum values at certain substrate temperature for different substrates, for example,  $750\text{ }^\circ\text{C}$  for Ti substrates [6] and  $860\text{ }^\circ\text{C}$  for Si substrates [28]. In the present work, such nucleation density may also increase with  $t$  from  $750\text{ }^\circ\text{C}$  to  $910\text{ }^\circ\text{C}$  on WC–6%Co substrates owing to the combined effects of the more  $[\text{CH}_3]$  radicals moving to the substrate surface and the enhanced surface energy. As a result, higher  $t$  induces a higher  $R$  in the thickness direction but a smaller  $G$  because of the competition of the high-density diamond crystals. In many previous investigations, the dependence of  $G$  on  $t$  is very different and even opposite, which may be caused by either different thicknesses of diamond films [9,20] or different deposition conditions (e.g., gas compositions, filament–substrate distance, substrate temperature range, total pressure range) [13,29].

The total pressure ( $p$ ) also plays an important role on  $R$  and  $G$  (Figs. 3(e<sub>3</sub>) and (f<sub>3</sub>)). Theoretically, it is well known that with the decrease in  $p$ , the mean free paths of the active  $[\text{CH}_3]$  and [H] radicals increase, for which they undergo fewer collisions when moving to the substrate surface and thus are more effective in the formation of the diamond nucleation and growth (also as depicted in Fig. 4) [30]. Such effect is similar to that when  $\phi$  or  $t$  increase, so  $G$  monotonically increases with  $p$  but  $R$  roughly drops off with  $p$  increasing from 1.6 to 4.0 kPa. Nevertheless,  $R$  slightly increases when  $p$  continues to increase from 4.0 to 6.0 kPa. The researches by SCHWARZ et al [14] gave the best correspondence to our results. A possible explanation was proposed that high-order carbon molecules formed at the high pressure tend to promote the diamond film growth. This phenomenon is much more obvious in MPCVD diamond films growth although the plasma density decreases as a function of  $p$ , and the arrival rate of active radicals at the substrate surface is lower at higher  $p$  [17,31].

In order to provide sufficient reactant gas in diamond films growth on inner hole surfaces, the methane and excessive hydrogen are pre-mixed and introduced into inner holes of the substrates with an inlet pipe placed just above the fixture holding a pair of substrates, as plotted in Fig. 5(a), which is similar to the model adopted in our previous studies [20]. Within the total mass flow ( $F$ ) used in this work (600–1000 mL/min), the velocity of the reactant gas in the inner hole is higher than 0.07 m/s, as shown in Fig. 5(b), adopting the published simulation method [20,21,32]. Such velocity is much higher than that close to the substrate surface with reactant gas totally free diffusing in the reactor. Under such special condition,  $R$  will slightly increase with  $F$ , since relatively higher  $F$  represents more reactant gas supply to provide more

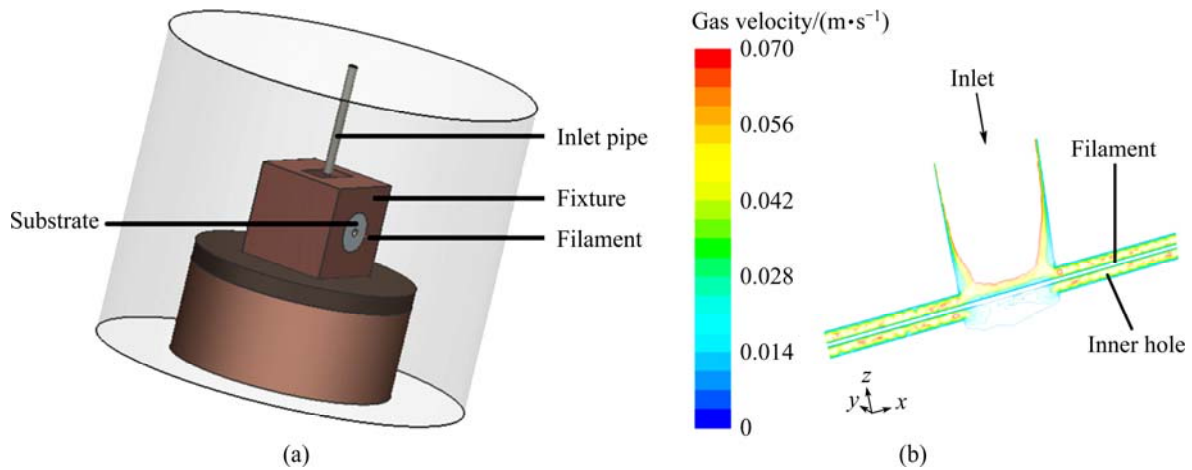


Fig. 5 Model of vacuum reactor (a) and simulated gas velocities in inner holes of substrates when  $F=600$  mL/min (b)

sufficient  $[\text{CH}_3]$  and  $[\text{H}]$  radicals for the diamond films growth. It has been proved that the increase in  $F$  can promote the secondary nucleation and crystal coalescence [6,33], and in diamond films growth with excessive argon as additional gas, the increase in  $F$  can develop closed film of NCD clusters [10]. Unexpectedly, in the present work,  $G$  also increases with  $F$ , probably owing to the effect of the relatively higher gas velocity caused by the special inlet position, which might inhibit the secondary nucleation to some extent while insuring the growth rate in the thickness direction.

### 3.2 Residual stress and structural quality

Raman spectroscopy was adopted within the diamond CVD community, given its ability to reveal the presence of different carbon phases (most notably diamond and graphite) [12]. The as-deposited diamond films with the same thickness ( $\sim 20$   $\mu\text{m}$ ) were all characterized by Raman spectroscopy, still at four different locations on each sample. The Raman spectra obtained in the present investigation show an obvious background that rises to higher wavenumber. So they are best fitted using a linear two-point line for the photoluminescence (PL) baseline subtraction and analyzed by Gauss-Lorentz (G-L) deconvolution integrated peaks. The representative spectra and corresponding peaks are all shown in Fig. 6, where the Raman-original data are the Raman spectra after the PL baseline subtraction; the Raman-fitting is the Raman spectra after the G-L fitting; AS is the fitted peak of the amorphous  $\text{sp}^3$  phase; DIA is the diamond phase; TP is the trans-polyacetylene; G is the graphitic band; D is the disordered carbon band.

The Raman spectra of diamond films can be adopted to assess their total residual stress ( $\sigma$ ), by analyzing the diamond peak shifts using the equation listed below [34]:

$$\sigma = -0.567(\nu - \nu_d) \quad (2)$$

where  $\nu$  is the wavenumber of the measured diamond peak;  $\nu_d$  is the wavenumber of the natural stress-free diamond peak ( $1332.4$   $\text{cm}^{-1}$ ). For all the films, positive shifts from  $\nu_d$  are obtained, indicating compressive residual stresses, manifesting as minus  $\sigma$  values. In the whole article, as-described higher  $\sigma$  will refer to the higher compressive residual stress (higher absolute value). The beam area of Raman spectroscopy is about  $1$   $\mu\text{m}$  in diameter in the present work, so it is realized that the Raman spectroscopy measures the relatively localized stresses by comparing with the X-ray and substrate curvature methods [35,36].

The Raman spectrum also allows the approximate assessment of the structural quality of the diamond film ( $Q$ ) from the ratio  $I_D/I_T$ , where  $I_D$  represents the integrated intensity of the diamond peak and  $I_T$  represents the total integrated intensity of all the peaks [9].

As presented in Table 2 and Fig. 3(c<sub>4</sub>),  $t$ ,  $\varphi$  and  $p$  seem to play important roles on  $\sigma$  and  $Q$ . The total residual stress ( $\sigma$ ) in the diamond film includes the thermal residual stress ( $\sigma_{\text{th}}$ ) and the growth residual stress ( $\sigma_g$ ). The former is caused by the difference between thermal expansion coefficients of the diamond ( $\alpha_d$ ) and substrate (WC-6%Co,  $\alpha_s$ ) during the cooling down process from  $t$  to room temperature, which can be calculated using the following equation [37]:

$$\sigma_{\text{th}} = \frac{E_d}{(1-\nu_d)} \times (t_R - t) \times (\alpha_s - \alpha_d) = \sum_i \frac{E_d}{(1-\nu_d)} \times (t_R - t_i) \times (\alpha_s - \alpha_d)_i \quad (3)$$

where  $E_d$  is the elastic modulus of the diamond;  $\nu_d$  is the Poisson ratio of the diamond;  $t_R$  is the room temperature;  $i$  means the interval. The three parameters ( $E_d$ ,  $\nu_d$  and  $t_R$ ) all keep constant in this work, so  $\sigma_{\text{th}}$  linearly increases with  $t$  considering that  $\alpha_s$  is always larger than  $\alpha_d$  in the

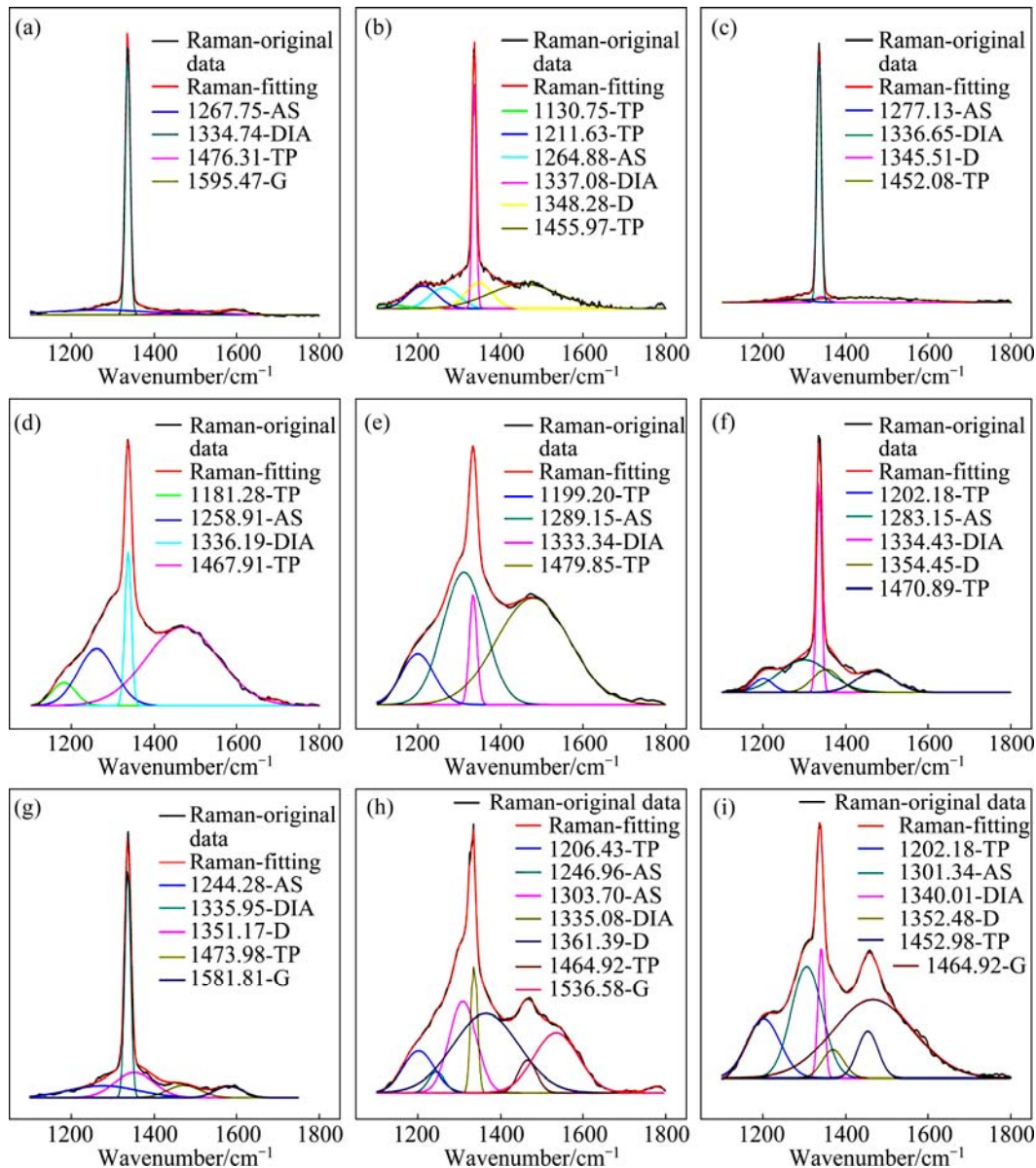


**Fig. 6** Raman spectra of as-deposited diamond films with same thickness ( $\sim 20 \mu\text{m}$ ): (a) No. 1; (b) No. 2; (c) No. 3; (d) No. 4; (e) No. 5; (f) No. 6; (g) No. 7; (h) No. 8; (i) No. 9

temperature range of  $0\text{--}1000 \text{ }^\circ\text{C}$ . It is supposed that the effect of  $T$  on  $\sigma$  mainly depends on its effect on  $\sigma_{\text{th}}$ . Consequently,  $\sigma$  also increases with  $t$ , indicating that higher  $t$  can induce higher compressive residual stress in the diamond film growth on the inner hole surface. However, the dependence of  $Q$  on  $t$  presents nonlinear variation. Because  $t$  is changed with the filament temperature in the present work, the increase in  $t$  from  $750$  to  $830 \text{ }^\circ\text{C}$  means increasing the filament temperature, for which more [H] radicals are produced [6]. The conversion rate of the chemisorbed  $[\text{CH}_3]$  radicals to carbon atoms by the abstracting of the [H] atoms is highly according to the Arrhenius law, and the gasification of the aromatic carbons by the [H] atoms becomes quicker while the deposition rate of non-diamond carbons becomes slower with an increase

in  $t$ . The condensing aromatic carbon molecules also convert into amorphous  $\text{sp}^2$  and  $\text{sp}^3$  hybridized carbonaceous networks [38]. Moreover, under the effects of [H] atoms and high  $t$  in an appropriate range, the  $\text{sp}^2$ -bonded carbon can convert to  $\text{sp}^3$ -bonded carbon [39]. For all the reasons, the increase in  $t$  from  $750$  to  $830 \text{ }^\circ\text{C}$  can improve the quality of the diamond film and  $830 \text{ }^\circ\text{C}$  might be defined as the most appropriate temperature for high-quality diamond films growth on inner hole surfaces of the WC-6% Co substrates. However, further increase in  $t$  from  $830$  to  $910 \text{ }^\circ\text{C}$  will result in  $Q$  deterioration, which should be attributed to the promoted growth of the amorphous carbon and the graphitic phase.

As shown in Figs. 3(c<sub>2</sub>) and (d<sub>2</sub>), with reducing  $\varphi$ ,  $\sigma$  will drop off, but  $Q$  will deteriorate unexpectedly. The growth residual stress ( $\sigma_{\text{g}}$ ) arises from either the

non-diamond phases or the defects in the diamond film and at the boundaries, like microtwins, dislocations, impurities, among others [40]. For example, due to the fact that the specific volume of the graphite is 1.5 times larger than that of the diamond, the graphitic carbon formed in the diamond film is responsible for the augment of the compressive residual stress [41]. It has been discussed above that the increase in  $[CH_3]$  radicals caused by the high concentration can promote the nucleation of diamond crystals, for which a little more non-diamond phases and defects tend to concentrate, and thus relatively higher  $\sigma_g$  or  $\sigma$  exist in as-deposited diamond films. However, the unexpected dependence of  $Q$  on  $\phi$  may be attributed to another reason: under the  $[H]$  atoms-rich atmosphere at relatively lower  $\phi$ ,  $[CH_3]$  radicals will easily react with  $[H]$  atoms to reform hydrocarbons [6]. Moreover, it will also lead to a high conversion rate from  $CH_4$  to  $C_2H_2$  [42] and change the compositions of as-deposited diamond films because the effect of  $C_2H_2$  on the growth of diamond is much less significant than  $[CH_3]$  [43], thus probably more H-related impurities will exist in as-deposited diamond films. This result is totally different from the previous study by ALI and ÜRGEN [44], demonstrating that by increasing  $\phi$ , the quality of the diamond film would gradually degrade due to either the condensing of aromatic hydrocarbons formed at relatively higher  $\phi$  or the slight decrease in production of  $[H]$  atoms in overall mass. The former can poison the film and promote the formation of amorphous carbon and the latter can reduce the etching rate of the graphite [44]. Such difference might be ascribed to the different deposition conditions, since in the confined inner hole space, the reaction between  $[CH_3]$  radicals and  $[H]$  atoms, the conversion from  $CH_4$  to  $C_2H_2$  and the formation of H-related impurities may play a momentous role in  $Q$  of as-deposited films when  $\phi$  is in the range of 1.5%–4.5%, which still need further investigations.

The total pressure ( $p$ ) also has significant effects on  $\sigma$  mainly by affecting the growth residual stress ( $\sigma_g$ ). It has been discussed above that when  $p$  is as low as 1600 Pa, mean free paths of active  $[CH_3]$  and  $[H]$  radicals are long enough to avoid them from undergoing many collisions when moving to substrate surfaces and promote the secondary nucleation. Therefore, more non-diamond phases and defects also tend to concentrate at the more grain boundaries and induce a rise in  $\sigma_g$  and  $\sigma$ . On the contrary, when  $p$  is as high as 6000 Pa, much more active radicals, especially  $[H]$  atoms will be produced by the heating of hot filaments and move to substrate surfaces so as to induce much more active sites on the deposited surfaces. Although the average grain size ( $G$ ) of the diamond crystals on the surface is larger than that when  $p=6000$  Pa due to the growing of a large

proportion of crystals, it is still supposed that slightly higher nucleation density, even more non-diamond phases and defects, higher  $\sigma_g$  and  $\sigma$  could be obtained at the initial growth stage. From Fig. 2 ( $p=6000$  Pa for experiment Nos. 3, 5, 7), it can also be observed that a small number of secondary nuclei still exist between the as-grown diamond crystals. Arising from similar reasons discussed above,  $Q$  performs the same  $p$  dependence as  $\sigma$ . Generally speaking, 4000 Pa is determined as the optimal  $p$  in the present work with the purpose of reducing  $\sigma$  and improving  $Q$  of as-deposited diamond films.

### 3.3 Adhesion and wear rate

The wear rates of diamond films with the same thickness ( $\sim 20$   $\mu\text{m}$ ) were obtained by wear tests, as depicted in Fig. 7. For the HFCVD diamond films deposited on inner hole surfaces, it is inconvenient to adopt conventional indentation or scratch methods to evaluate their adhesion, so their lifetime in the wear tests, defined as the start time of the film delamination and removal, is applied as a criterion of the adhesion ( $\delta$ ). The wear rates of most the diamond films present a typical steady stage. The average wear rate in such stage ( $I_{da}$ ) is calculated as the total mass loss divided by the load (3400 N) and the total sliding distance. The values of  $\delta$  and  $I_{da}$  are shown in Table 2 and their dependence on the deposition parameters are plotted in Fig. 3.

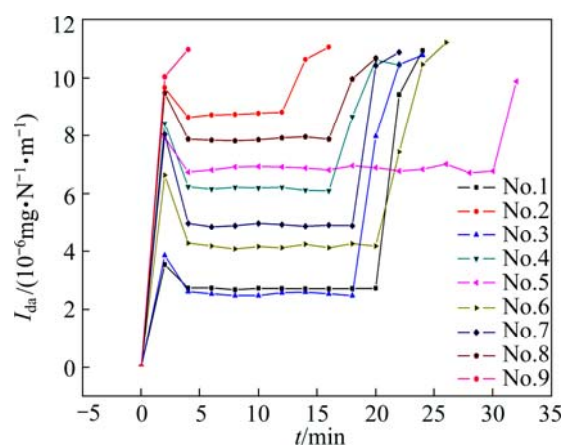


Fig. 7 Wear rates of diamond films with same thickness ( $\sim 20$   $\mu\text{m}$ ) obtained by wear tests

It has been indicated that the presence of the compressive residual stress in as-deposited diamond films generally has strong effects on  $\delta$ , which can prevent cracks initiated at the surface to propagate to the interface to form vertical cracks but promote crack paths parallel to the interface [45]. Under the sliding condition of the wear test in the present work, the radial load between the wire and the diamond film can induce some shear stresses and microcracks at the depth close to the interface between the film and the substrate. Although

the higher compressive  $\sigma$  can slow down the propagation of surface cracks to the interface, the propagation of the microcracks along the interface and the formation of the parallel cracks will be sped up. Especially, the diamond films with high  $\sigma$  are much easier to be removed from substrates once the vertical cracks intersect with the parallel cracks. Generally speaking, compressive stresses in the diamond films in the present work are supposed to promote film delamination from the substrate [12]. As a result,  $\delta$  presents almost the same dependence with the deposition parameters as  $\sigma$ , except that when  $p$  is as high as 6000 Pa, which should be attributed to the effect of  $G$ . Such  $p$  will cause a little higher  $\sigma$  than that when  $p=4000$  Pa, but it is supposed that the relatively larger diamond crystals formed under higher  $p$  can enhance the mechanical bonding between the film and the substrate [46].

Irrespective of the lifetime of the different diamond films, the steady-state wear rate ( $I_{da}$ ) almost exclusively has a close relationship with  $Q$ , because decreasing  $Q$  means the reduction of the diamond phase owning high hardness and excellent wear behavior, inducing a certain deterioration of the hardness and wear resistance of the whole diamond film. Consequently,  $I_{da}$  presents almost the inverse dependence with the deposition parameters by comparison with  $Q$ . It must be mentioned that there are some deviations when  $\varphi=4.5\%$  and  $F=800$  mL/min, owing to the influence of the  $I_{da}$  value in the experiment No. 4, which is approximately defined as  $10 \times 10^{-6}$  mg/(N·m) because such diamond film with the worst adhesion is rapidly removed from the substrate after only 2 min test. This value might be greater than its actual  $I_{da}$  value if no large-area film removal occurs.

### 3.4 Deposition parameters optimization

As obtained by the Taguchi method, the dependence of the six indexes on the four controllable factors is diverse. The goal in the diamond film growth on the inner hole surface is to obtain a diamond film with the highest  $R$ ,  $Q$  and  $\delta$ , while minimizing the  $G$ ,  $\sigma$  and  $I_{da}$ . In

terms of the defining method proposed in the study by SALGUEIREDO et al [9], a new figure-of-merit (FOM,  $f_m$ ) is defined to comprehensively access the film valuation and determine the optimal deposition parameters:

$$f_m = \left| \frac{R \times Q \times \delta}{G \times \sigma \times I_{da}} \right| \quad (4)$$

FOMs for the nine diamond films are respectively calculated as: 145, 6.34, 101, 5.75, 11.7, 110, 35.15, 2.10 and 1.24. The influences of the deposition parameters on FOM and corresponding ranges are presented in Fig. 8. It is obvious that  $t$ ,  $\varphi$  and  $p$  all have significant effects on FOM, and the largest FOM is probably obtained at the medium  $t$ ,  $\varphi$ ,  $F$  and the highest  $\varphi$  within considered deposition condition ranges in the present work, indicating diamond films with the best comprehensive properties.

The optimized deposition parameters are listed as follows:  $t=830$  °C,  $\varphi=4.5\%$ ,  $p=4000$  Pa and  $F=800$  mL/min, which are similar to those in experiment No.1, just increasing  $\varphi$  from 3.0% to 4.5%. Based on the same deposition and characterization methods, the HFCVD diamond film deposited with the optimized parameters does show even more favorable properties:  $R=4.417$   $\mu\text{m}/\text{h}$ ,  $G=4.855$   $\mu\text{m}$ ,  $\sigma=-1.644$  GPa,  $Q=48.22\%$ ,  $\delta=20$  min,  $I_{da}=2.76 \times 10^{-6}$  mg/(N·m),  $f_m=193.37$ .

It is supposed that the conclusions in the present work can apply to HFCVD diamond films growth on inner hole surfaces within certain realms of diameters (2.0–20 mm), but there might be some differences for inner holes with ultra large or ultra small diameters. However, the proposed optimization method based on the orthogonal simulations is universal for the inner holes with any diameters and shapes, even the complicated external surfaces. Moreover, based on the different concerned properties of as-deposited diamond films for different applications, the FOM can be redefined in order to describe the comprehensive performance much closer to the actual condition.

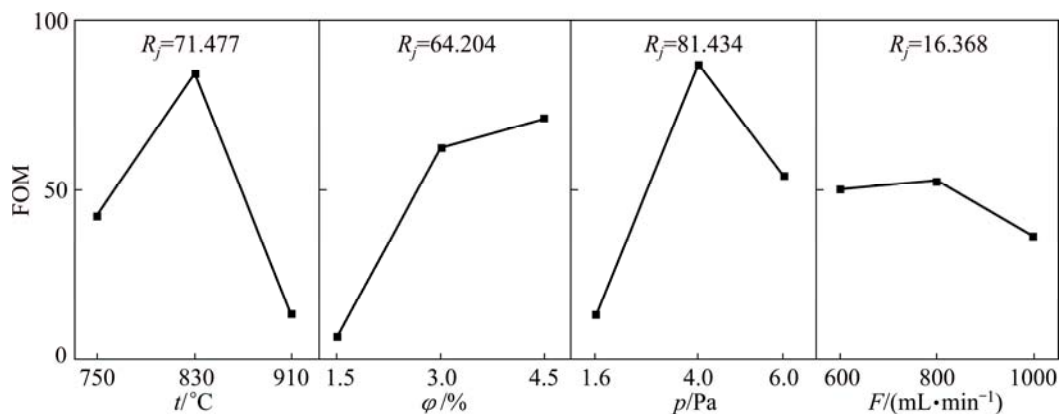


Fig. 8 Influences of controllable factors on FOM and corresponding ranges

## 4 Conclusions

1) With increasing either the substrate temperature ( $t$ ) or the carbon content ( $\phi$ ), the growth rate ( $R$ ) significantly rises, but the grain size ( $G$ ) drops off.  $G$  also monotonically increases with the total pressure ( $p$ ). Nevertheless,  $R$  roughly decreases with  $p$  increasing from 1600 to 4000 Pa, but slightly increases when  $p$  continues to increase to 6000 Pa. The increase in the total mass flow ( $F$ ) can promote both the growth rate of the diamond film in the thickness direction and the crystals growing up.

2) The total residual stress ( $\sigma$ ) linearly increases with  $t$ , but relatively higher or lower  $t$  as compared with 830 °C both result in  $Q$  deterioration. Higher  $\sigma$  exists in diamond films fabricated with higher  $\phi$ , which surprisingly present better  $Q$ . A medium  $p$  of 4000 Pa can provide diamond films with relatively lower  $\sigma$  and better  $Q$ .

3) The  $\sigma$  has strong effects on the adhesion ( $\delta$ ) between the diamond film and substrate. So,  $\delta$  presents almost the same dependence with the deposition parameters as  $\sigma$ , except that when  $p$  is as high as 6000 Pa. The steady-state wear rate ( $I_{da}$ ) has a close relationship with  $Q$ , which performs almost the inverse dependence with the deposition parameters by comparison with  $Q$ .

4) A new figure-of-merit (FOM) is defined to comprehensively evaluate the HFCVD diamond film and optimize the deposition parameters, aiming to deposit a diamond film with the highest  $R$ ,  $Q$  and  $\delta$ , while minimizing the  $G$ ,  $\sigma$  and  $I_{da}$ . Within the considered deposition condition ranges, optimal deposition parameters are finally determined as:  $t=830$  °C,  $\phi=4.5\%$ ,  $p=4000$  Pa and  $F=800$  mL/min.

## References

- [1] SUN F H, MA Y P, SHEN B, ZHANG Z M, CHEN M. Fabrication and application of nano-microcrystalline composite diamond films on the interior hole surfaces of Co cemented tungsten carbide substrates [J]. *Diamond and Related Materials*, 2009, 18: 276–282.
- [2] WHEELER D W, WOOD R J K, HARRISON D, SMITH E. Application of diamond to enhance choke valve life in erosive duties [J]. *Wear*, 2006, 261: 1087–1094.
- [3] WANG X C, ZHANG J G, SUN F H, ZHANG T, SHEN B. Investigations on the fabrication and erosion behavior of the composite diamond coated nozzles [J]. *Wear*, 2013, 304: 126–137.
- [4] ABREU C S, AMARAL M, FERNANDES A J S, OLIVEIRA F J, SILVA R F, GOMES J R. Friction and wear performance of HFCVD nanocrystalline diamond coated silicon nitride ceramics [J]. *Diamond and Related Materials*, 2006, 15: 739–744.
- [5] BACHMANN P, ENCKEVORT W V. Diamond deposition technologies [J]. *Diamond and Related Materials*, 1992, 1: 1021–1034.
- [6] GUO L, CHEN G H. High-quality diamond film deposition on a titanium substrate using the hot-filament chemical vapor deposition method [J]. *Diamond and Related Materials*, 2007, 16: 1530–1540.
- [7] RATS D, VANDENBULCKE L, HERBIN R, BENOIT R, ERRE R, SERIN V, SEVELY J. Characterization of diamond films deposited on titanium and its alloys [J]. *Thin Solid Films*, 1995, 270: 177–183.
- [8] MAY P W, ASHFOLD M N R, MANKELEVICH Y A. Microcrystalline, nanocrystalline, and ultrananocrystalline diamond chemical vapor deposition: Experiment and modeling of the factors controlling growth rate, nucleation, and crystal size [J]. *Journal of Applied Physics*, 2007, 101: 1–9.
- [9] SALGUEIREDO E, AMARAL M, NETO M A, FERNANDES A J S, OLIVEIRA F J, SILVA R F. HFCVD diamond deposition parameters optimized by a Taguchi Matrix [J]. *Vacuum*, 2011, 85: 701–704.
- [10] AMARAL M, FERNANDES A J S, VILA M, OLIVEIRA F J, SILVA R F. Growth rate improvements in the hot-filament CVD deposition of nanocrystalline diamond [J]. *Diamond and Related Materials*, 2006, 15: 1822–1827.
- [11] LI L, LI H D, LU X Y, CHENG S H, WANG Q L, REN S Y, LIU J W, ZOU G T. Dependence of reaction pressure on deposition and properties of boron-doped freestanding diamond films [J]. *Applied Surface Science*, 2010, 256: 1764–1768.
- [12] WEI Q, ASHFOLD M N R, MANKELEVICH Y A, YU Z M, LIU P Z, MA L. Diamond growth on WC-Co substrates by hot filament chemical vapor deposition: Effect of filament–substrate separation [J]. *Diamond and Related Materials*, 2011, 20: 641–650.
- [13] WEI Q, YU Z M, MA L, YIN D F, YE J. The effects of temperature on nanocrystalline diamond films deposited on WC–13wt.%Co substrate with W–C gradient layer [J]. *Applied Surface Science*, 2009, 256: 1322–1328.
- [14] SCHWARZ S, ROSIHAL S M, FRANK M, BREIDT D, SINGER R F. Dependence of the growth rate, quality, and morphology of diamond coatings on the pressure during the CVD-process in an industrial hot-filament plant [J]. *Diamond and Related Materials*, 2002, 11: 589–595.
- [15] YU Z, FLODSTROM A. Pressure dependence of growth mode of HFCVD diamond [J]. *Diamond and Related Materials*, 1997, 6: 81–84.
- [16] TAHER M A, SCHMIDT W F, NASEEM H A, BROWN W D, MALSHE A P, NASRAZADANI S. Effect of methane concentration on physical properties of diamond-coated cemented carbide tool inserts obtained by hot-filament chemical vapour deposition [J]. *Journal of Materials Science*, 1998, 33: 173–182.
- [17] LI X, PERKINS J, COLLAZO R, NEMANICH R J, SITAR Z. Investigation of the effect of the total pressure and methane concentration on the growth rate and quality of diamond thin films grown by MPCVD [J]. *Diamond and Related Materials*, 2006, 15: 1784–1788.
- [18] HIRAKURI K K, KOBAYASHI T, NAKAMURA E, MUTSUKURA N, FRIEDBACHER G, MACHI Y. Influence of the methane concentration on HF-CVD diamond under atmospheric pressure [J]. *Vacuum*, 2001, 63: 449–454.
- [19] SUN F H, ZHANG Z M, CHEN M, SHEN H S. Improvement of adhesive strength and surface roughness of diamond films on Co-cemented tungsten carbide tools [J]. *Diamond and Related Materials*, 2003, 12: 711–718.
- [20] WANG X C, ZHANG T, SHEN B, ZHANG J G, SUN F H. Simulation and experimental research on the substrate temperature distribution in HFCVD diamond film growth on the inner hole surface [J]. *Surface and Coatings Technology*, 2013, 219: 109–118.
- [21] WANG X C, ZHANG J G, ZHANG T, SHEN B, SUN F H. Simulation optimization of the heat transfer conditions in HFCVD diamond film growth on the inner hole surfaces [J]. *Surface Review and Letters*, 2013, 20: 1–13.
- [22] MAY P W, HARVEY J N, ALLAN N L, RICHLEY J C, MANKELEVICH Y A. Simulations of chemical vapor deposition diamond film growth using a kinetic Monte Carlo model [J]. *Journal*

- of Applied Physics, 2010, 108: 1–12.
- [23] MAY P W, MANKELEVICH Y A. From ultrananocrystalline diamond to single crystal diamond growth in hot filament and microwave plasma-enhanced CVD reactors: A unified model for growth rates and grain sizes [J]. Journal of Physical Chemistry C, 2008, 112: 12432–12441.
- [24] WEI Q, YU Z M, ASHFOLD M N R, CHEN Z, WANG L, MA L. Effects of thickness and cycle parameters on fretting wear behavior of CVD diamond coatings on steel substrates [J]. Surface and Coatings Technology, 2010, 205: 158–167.
- [25] SMITH J A, CAMERON E, ASHFOLD M N R, MANKELEVICH Y A, SUETIN N V. On the mechanism of CH<sub>3</sub> radical formation in hot filament activated CH<sub>4</sub>/H<sub>2</sub> and C<sub>2</sub>H<sub>2</sub>/H<sub>2</sub> gas mixtures [J]. Diamond and Related Materials, 2001, 10: 358–363.
- [26] KONDOH E, TANAKA K, OHTA T. Reactive-flow simulation of the hot-filament chemical-vapor deposition of diamond [J]. Journal of Applied Physics, 1993, 74: 4513–4520.
- [27] HAYASHI K, YAMANAKA S, WATANABE H, SEKIGUCHI T, OKUSHI H, KAJIMURA K. Diamond films epitaxially grown by step-flow mode [J]. Journal of Crystal Growth, 1998, 183: 338–346.
- [28] HAYASHI Y, DRAWL W, MESSIER R. Temperature dependence of nucleation density of chemical vapor deposition diamond [J]. Japanese Journal of Applied Physics, 1992, 31: 193–196.
- [29] BARBOSA D C, ALMEIDA F A, SILVA R F, FERREIRA N G, TRAVA-AIROLDI V J, CORAT E J. Influence of substrate temperature on formation of ultrananocrystalline diamond films deposited by HFCVD argon-rich gas mixture [J]. Diamond and Related Materials, 2009, 18: 1283–1288.
- [30] SARANGI S K, CHATTOPADHYAY A, CHATTOPADHYAY A K. Effect of pretreatment methods and chamber pressure on morphology, quality and adhesion of HFCVD diamond coating on cemented carbide inserts [J]. Applied Surface Science, 2008, 254: 3721–3733.
- [31] STERNSCHULTE H, BAUER T, SCHRECK M, STRITZKER B. Comparison of MWPCVD diamond growth at low and high process gas pressures [J]. Diamond and Related Materials, 2006, 15: 542–547.
- [32] ZHANG T, WANG X C, SHEN B, SUN F H, ZHANG Z M. The effect of deposition parameters on the morphology of micron diamond powders synthesized by HFCVD method [J]. Journal of Crystal Growth, 2013, 372: 49–56.
- [33] SONG G H, SUN C, HUANG R F, WEN L S. Simulation of the influence of the filament arrangement on the gas phase during hot filament chemical vapor deposition of diamond films [J]. Journal of Vacuum Science and Technology A, 2000, 18: 860–863.
- [34] RALCHENKO V G, SMOLIN A A, PEREVERZEV V G, OBRAZTSOVA E D, KOROTOUSHENKO K G, KONOV V I, LAKHOTKIN Y V, LOUBNIN E N. Diamond deposition on steel with CVD tungsten intermediate layer [J]. Diamond and Related Materials, 1995, 4: 754–758.
- [35] KUO C T, LIN C R, LIEN H M. Origins of the residual stress in CVD diamond films [J]. Thin Solid Films, 1996, 290–291: 254–259.
- [36] CHEN S L, SHEN B, ZHANG J G, WANG L, SUN F H. Evaluation on residual stresses of silicon-doped CVD diamond films using X-ray diffraction and Raman spectroscopy [J]. Transactions of Nonferrous Metals Society of China, 2012, 22(12): 3021–3026.
- [37] AMIRHAGHI S, REEHAL H S, WOOD R J K, WHEELER D W. Diamond coatings on tungsten carbide and their erosive wear properties [J]. Surface and Coatings Technology, 2001, 135: 126–138.
- [38] FRENKLACH M, WANG H. Detailed surface and gas-phase chemical kinetics of diamond deposition [J]. Physical Review B, 1991, 43: 1520–1545.
- [39] SINGH J. Novel techniques for selective diamond growth on various substrates [J]. Journal of Materials Engineering and Performance, 1994, 3: 378–385.
- [40] FERREIRA N G, ABRAMOF E, LEITE N F, CORAT E J, TRAVA-AIROLDI V J. Analysis of residual stress in diamond films by X-ray diffraction and micro-Raman spectroscopy [J]. Journal of Applied Physics, 2002, 91: 2466–2472.
- [41] VILA M, AMARAL M, OLIVEIRA F J, SILVA R F, FERNANDES A J S, SOARES M R. Residual stress minimum in nanocrystalline diamond films [J]. Applied Physics Letters, 2006, 89: 1–3.
- [42] RUF B. Simulation of reactive flow in filament-assisted diamond growth including hydrogen surface chemistry [J]. Journal of Applied Physics, 1996, 79: 7256–7263.
- [43] PARK S. Numerical modeling of diamond growth environment in HFCVD reactors [J]. Metals and Materials, 1999, 5: 225–229.
- [44] ALI M, ÜRGEN M. Surface morphology, growth rate and quality of diamond films synthesized in hot filament CVD system under various methane concentrations [J]. Applied Surface Science, 2011, 257: 8420–8426.
- [45] GUNNARS J, ALAHELISTEN A. Thermal stresses in diamond coatings and their influence on coating wear and failure [J]. Surface and Coatings Technology, 1996, 80: 303–312.
- [46] SHARDA T, RAHAMAN M M, NUKAYA Y, SOGA T, JIMBO T, UMENO M. Structural and optical properties of diamond and nano-diamond films grown by microwave plasma chemical vapor deposition [J]. Diamond and Related Materials, 2001, 10: 561–567.

## 沉积参数对 WC-Co 基体内孔 HFCVD 金刚石薄膜生长的影响

王新昶, 林子超, 沈彬, 孙方宏

上海交通大学 机械与动力工程学院, 上海 200240

**摘要:** 在内孔 HFCVD 金刚石薄膜沉积过程中, 沉积温度( $t$ )、碳源浓度( $\varphi$ )、总反应压力( $p$ )和气体总流量( $F$ )等沉积参数对金刚石薄膜的生长具有显著影响。采用 Taguchi 方法系统研究这 4 个关键参数对内孔 HFCVD 金刚石薄膜性能的综合影响, 并且通过自定义的品质因数(figure-of-merit, FOM)评价金刚石薄膜的综合性能。沉积温度、碳源浓度和总反应压力对于内孔 HFCVD 金刚石薄膜的各项性能及 FOM 均存在显著影响, 并且与平片或外表面沉积存在一定的差异。根据上述影响性分析的结果, 以获得最佳的内孔 HFCVD 金刚石薄膜综合性能为优化目标所确定的最优化沉积参数为:  $t=830\text{ }^{\circ}\text{C}$ ,  $\varphi=4.5\%$ ,  $p=4000\text{ Pa}$ ,  $F=800\text{ mL/min}$ 。

**关键词:** HFCVD 金刚石薄膜; 内孔表面; Taguchi 方法; 沉积参数; 优化

(Edited by Yun-bin HE)